

## Estimation of the relative active tectonics in Shahriary basin (Central Iran) using geomorphic and seismicity indices

**Alireza Habibi\***; MSc. Researcher, Soil Conservation and Watershed Management Research Institute, Tehran, Iran.

**Mohammadreza Gharibreza**; Assistance Professor, Soil Conservation and Watershed Management Research Institute, Tehran, Iran.

Received: June 25, 2014 - Accepted: October 5, 2015

### Abstract

Iran is well known for having countless historical and instrumental records of tectonic events. Shahriary catchment, as a study area, is part of the Zagros collision seismic province. This research aimed to introduce a new method which is useful in identifying the relative active tectonic events of an area. The research method was designed in order to calculate the relative active tectonic index (IRAT) using geomorphic and seismicity indices. Accordingly, IRAT was determined based on the river length–gradient index (SL), drainage basin asymmetry (AF), transverse topographic symmetry factor (TP), hypsometric integral (HI) and the drainage basin shape index (BS). The obtained results showed that areas with relatively high, moderate and low tectonic activities comprised 71%, 19% and 10% of the study area, respectively. In addition, the calculated mean seismicity in Shahriary was  $4.8 \pm 0.2$  Ms, with an acceleration gravity of 0.3 g (i.e., a high-risk zone). The resultant data confirmed the ability of seismicity indices to estimate IRATs. Therefore, application of the proposed method for assessing the IRAT of an area is confidently recommended in watershed management planning.

### Keywords

geomorphic indices, relative active tectonics, seismic, Shahriary.

## 1. Introduction

Earthquakes, as one of the most dangerous geo-induced events in Iran, result in extensive destruction and affect a large number of people. Iran is divided into 20 seismic provinces, some of which are known as neotectonic areas (IIEES, 1995). Vladimir Obruchev (1984) defined the term *Neotectonics* as "recent tectonic movements which occurred in the upper part of Tertiary (Neogene) and in the Quaternary, and which played an essential role in the origin of the contemporary topography". In addition, such areas represent a clear correlation between morphological features and tectonic activities (Keller and Pinter, 2002). Recently, geomorphic indices have been widely used in evaluating tectonic activities worldwide (Azor et al., 2002; Bull and McFadden, 1977; Keller and Pinter, 2002; Silva et al., 2003; Molin et al., 2004). On the other hand, the overall geometry of catchment, faults function and evidences of recent fault activity can be investigated by the drainage patterns (Maroukian et al., 2008). Della-Seta et al. (2008) believed that IRAT index was an indicator of morphotectonic features and landforms useful in the interpretation of tectonic events of an area., which are useful Bull and McFadden (1977) utilized the valley width to valley height ratio (VF) and an index of mountain sinuosity (SMF) in the evaluation of the IRAT. Similarly, Silva et al. (2003) linked tectonic activity in southern Spain to the VF, SMF and basin shape (BS) indices. Recently, El-Hamdouni et al. (2008) developed and applied a model that included the hypsometric integral (Hi), the stream

---

\* Corresponding Author, Email: habibi1354@yahoo.com

length–gradient index (SL), the IRAT and the previously developed indices. Iranian researchers have often utilized geomorphic indices in identifying the tectonic activities in different regions (Negaresh, 2003; Yamani et al., 2011; Madadi et al., 2005; Goorabi, 2007; Habibollah, 2007; Mokhtari, 2005; Khosravi, 2008; Khatib 2008; Karami, 2009; Zare-Mehrjerdi, 2012). At the moment, there are no previous literatures regarding the use of seismic indices to determine geomorphic indices. Thus, the aim of this research was to introduce a new method which will be useful in showing relative active tectonic events of an area by applying geomorphic and seismicity indices.

## 2. Study Area

The study area is located in the Zagros collision zone, known as neotectonic area. The total area of the Shahriary catchment is 15.7 km<sup>2</sup>. This catchment is located between 54° 13' and 54° 22' longitude and between 29° 32' and 29° 42' latitude. The stratigraphy of the Shahriary basin includes Devonian, Triassic, Eocene and Quaternary rock units. The lower and upper contacts of the rock units represent un-conformities and surface ruptures. In addition, ancient tectonic activities (Cimmerian and Laramide orogenic events) are known to have manifested in the petrography of the rock units. Here, the uplifting of metamorphic rock resulted in several erosive features and in the deposition of thick sequences during the quaternary period. Paul et al. (2010) reported the presence of two main faults, which were exposed from north to south (N-S) and northwest to southeast (NW-SE) in the study area. The longest which had a surface rupture of about 11 km occurred N-S and across the Quaternary stratigraphic units (Fig. 1). Several landforms, such as severely uplifted rocks, cliffs, dip-slip slopes, rock-falls and coarse-grained alluvial fans, were used to evaluate the IRAT with geomorphic indices.

## 3. Materials and Methods

### 3.1. Geomorphic indices

Quantitative geomorphic indices such as stream length gradient index (SL), the geological strength levels, asymmetric factor (AF), hypsometric integral (Hi), transverse topographic symmetry factor (Tp), index of drainage basin shape (Bs), and index of relative active tectonic (IRAT) were used to identify areas experiencing rapid tectonic deformation. Indeed, the capability of these indices, accompanied with seismicity indices, was tested in order to reveal natural hazards in a catchment.

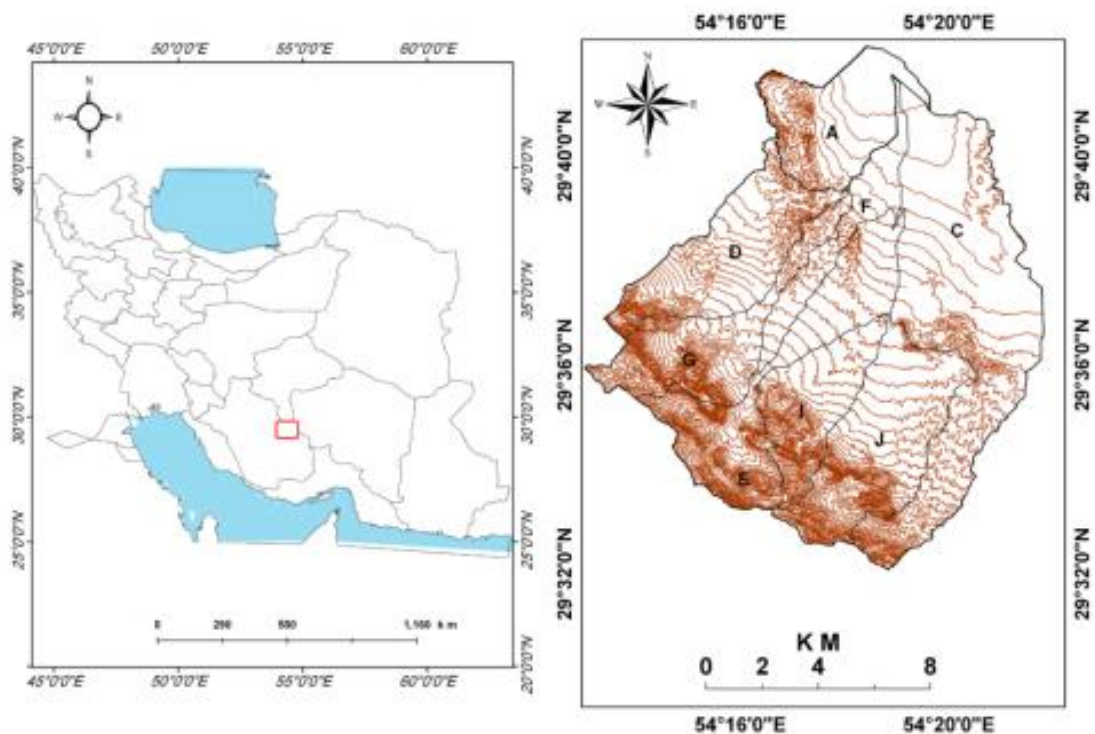


Fig. 1. The geographical position of Shahriary Catchment and its subcatchment

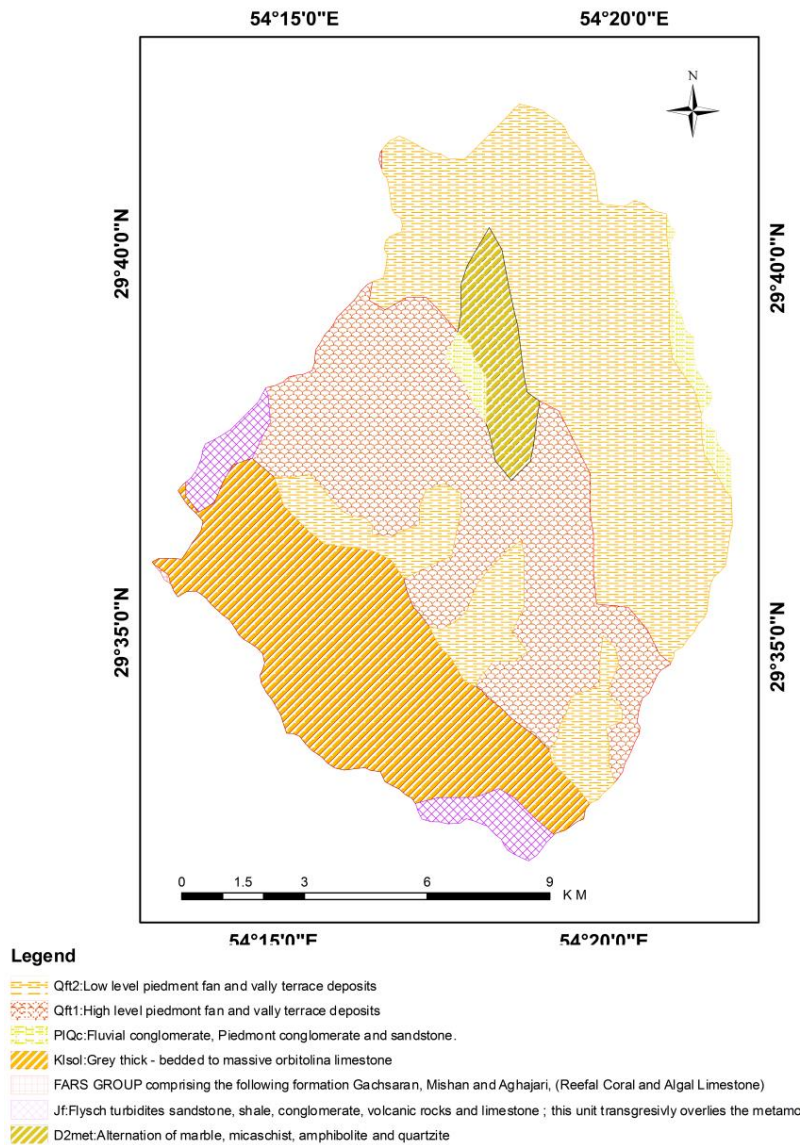


Fig. 2. The geological rock units of Shahriary catchment

### 3. 1. 1. Stream length gradient index (SL)

A river system can be a useful indicator for basin topography and geology. In addition, the drainage pattern and form of a river reveals the structural evolution of a basin. Therefore, Hack (1973) proposed the use of the stream length gradient (SL) in evaluating the effects of tectonics on river forms and drainage patterns. Variations in the SL index (Troiani and Della-Seta, 2008) were dependent on the local uplift and incipient local response of the index to regional tectonic events. This index was formulated by Hack (1973) as follows:

$$SL = \left( \frac{\Delta H}{\Delta L} \right) \times L \quad (1)$$

where  $\Delta H/\Delta L$  represents the local slope of the evaluated channel segment and  $L$  represents the channel length from the division the midpoint before reaching the channel. The SL classification (El-Hamdooni et al., 2008) comprised the following: Class (1), high tectonic activity with  $SL > 500$ ; Class (2), moderate tectonic activity with  $300 \leq SL < 500$ ; and Class (3), minor tectonic activity with  $SL < 300$ . This index was calculated by applying Equation 1 (with the ArcGIS 9.3 software) and data were extracted from a topographic map (1:25,000 scales).

### 3. 1. 2. The geological strength levels

In addition to the SL index results, the effects of rock resistance were evaluated based on the

average rock strengths. The rock strength allows for the identification of indication rock consolidation. Therefore, a very low strength corresponded to poorly consolidated sediments, such as alluvial deposits. El-Hamdooni et al. (2008) classified the geological strength of the rock units into four categories, including high strength, moderate strength, low strength and very low strength.

### 3. 1. 3. Asymmetric factor (AF)

The asymmetric factor (AF) was used in evaluating the existence of tectonics at a drainage basin scale. Its area of application is relatively large (Hare and Gardner, 1985; Keller and Pinter, 2002). The AF index is formulated as follows:

$$AF = 100 \times \left( \frac{A_r}{A_t} \right) \quad (2)$$

where  $A_r$  represents the area on the right side of the trunk stream and  $A_t$  represents the total area of the drainage basin. The  $A_r$  classification comprised two classes: Class (1), little or no basin tilting with  $AF \leq 50$ ; and Class (2), tilting or the effects of other tectonic events with  $AF \geq 50$ .

### 3. 1. 4. Hypsometric integral (Hi)

The Hi index was initially introduced by Strahler (1952) to indicate the elevation of a special area or landscape. The following equations were used to calculate the Hi index (Pike and Wilson, 1971; Mayer, 1990).

$$Hi = \left( H_{Ave} - H_{min} \right) / \left( H_{max} - H_{min} \right) \quad (3)$$

where  $H_{ave}$ ,  $H_{min}$  and  $H_{max}$  represents the average, minimum and maximum elevations, respectively. A digital elevation model (DEM) was used to calculate the required values. The Hi index classes comprised the following: Class (1) with  $Hi > 0.5$ ; Class (2) with  $0.4 < Hi < 0.5$ ; and Class (3) with  $< 0.4$ .

### 3. 1. 5. Transverse topographic symmetry factor (Tp)

The Tp index was introduced to evaluate the extent of tilting due to active tectonics (Alipoor et al., 2011). This index is represented as follows:

$$Tp = Da / Dd \quad (4)$$

where  $Da$  represents the distance from the midline of a basin to the main river axes and  $Dd$  represents the distance between the mid-line and the boundary of the drainage basin. The Tp value ranged between zero (minimum) and one (maximum).

### 3. 1. 6. Drainage basin shape index (Bs)

Relative active tectonic of an area is an indicator of the drainage basin shape (Bs) (Bull and McFadden, 1997). Higher Bs indices represented a stretched basin. Conversely, a circular basin presented few reactive tectonic effects or a more mature basin. Cannon (1976) and Ramirez-Herrera (1998) proposed using the Bs index for the horizontal projection of basin shape. The Bs index is expressed by the following equation:

$$Bs = Bl / Bw \quad (5)$$

where  $Bl$  represents the basin length from the headwaters to the mouth and  $Bw$  represents the width at its widest point. The following classes are included in the Bs groups (El-Hamdouni et al., 2008): Class (1), elongate basin with  $Bs > 4$ ; Class (2), semi-elongate basin with  $3 \leq Bs < 4$ ; and Class (3), circular basin with  $Bs < 3$ .

### 3. 1. 7. Relative active tectonics index (IRAT)

In previous research, the most important and widely used geomorphic index was that of the relative active tectonics (IRAT) (El-Hamdooni et al., 2008; Alipoor et al., 2011; Mahmood and Gloaguen, 2012). This index represented a summary and average of the given geomorphic indices that were used in a study as follows:

$$IRAT = S/N \quad (6)$$

where S represents the sum of the previous indices and N represents the number of selected indices. The IIRAT index was developed by El-Hamdooni et al. (2008) for different studies based on the topographic conditions of a basin. The following classes were used in the IRAT index: Class (1), very high with  $1.0 \leq IRAT < 1.5$ ; Class (2), high with  $1.5 \leq IRAT < 2.0$ ; Class (3), moderate with  $2.0 \leq IRAT < 2.5$ ; and Class (4), low with  $IRAT < 2.5$ .

### 3. 2. Seismic indices

#### 3. 2. 1. Estimated earthquake magnitude (Ms)

Seismicity indices are useful in indicating the size of the largest earthquake which will cause a particular fault. Therefore, the fault rupture demonstrates the future earthquake potential and earthquake size. Several well-tested empirical methods have been used in Iran (Mohajer-Ashjaei and Nowroozi, 1979; Nowroozi, 1985; Wells and Coppersmith, 1994) to estimate the Ms in various study areas. Thus, Equation 7, presented by Mohajer-Ashjaei and Nowroozi (1979), was on the basis of half of the fault length (LR) in km:

$$Ms = 5.4 + \text{LogLR} \quad (7)$$

Nowroozi's equation (1985) was proposed for faults of less than 85 km in length:

$$Ms = 1.259 + 1.244 \text{LogLR} \quad (8)$$

Similarly, Wells and Coppersmith (1994) suggested another empirical equation for estimating earthquake size based on surface rupture (km):

$$Ms = 5.08 + 1.16 \text{LogRL} \quad (9)$$

#### 3. 2. 2. Joint study

This is one of the most important field surveys of hard rock fractures. Cracks occur as a result of the displacement associated with the opening of the fracture being greater than the displacement due to lateral movement (Mandl, 2005). Joint study is prerequisite of the relative active tectonics of an area in order to show the rock strength and morphotectonic landform creation. The main directions of the tectonic stress on the rocks are shown in rose diagrams.

## 4. Results and Discussion

### 4. 1. Geomorphic characteristics

The SL index ranged between 179 and 411, and was largest in the southern region of the catchment. In the study area, this index was directly correlated with the geological strength. For example, an SL index of 411 (Fig. 2) occurred where the rock units had the greatest geological strength (Class 2). In addition, the Quaternary deposits had several fault ruptures with SL index values that were classified as Class 3 ( $SL < 300$ ).

The Bs index ranged from 1.17 to 4.64 within the study area (Fig. 3). Class 1 ( $Bs > 4$ ) included sub-catchments F and C which had Bs index values of 4.64 and 4.04, respectively. These sub-catchments comprised a distinct elongated shape and were crossed by the longest fault. However, sub-catchment A (classified as Class 3 ( $Bs < 3$ )) was circular with minor tectonic evidences.

The maximum and minimum indices of transverse topographic symmetry (Tp) values were 0.86 and 0.33, respectively. According to Alipoor et al. (2011), a Tp index of 1 indicated the area with the greatest tectonic activity. Similarly, the greatest distance between the stream centerlines and the main axes of the basin for the D and I sub-catchments corresponded to the highest Tp values (Fig. 4).

In the study area, the asymmetric factor (AF) varied between 2.38 and 20.09 (Fig. 5). The highest AF values were observed within the E and G sub-catchments, where the frequencies of the Ar/At ratio were 70 and 35.3 m, respectively. Therefore, these areas experienced greater tectonic movements. In contrast, Class 3 ( $AF < 7$ ) included the A, F, I and J sub-catchments, which represented the relative asymmetry factors.

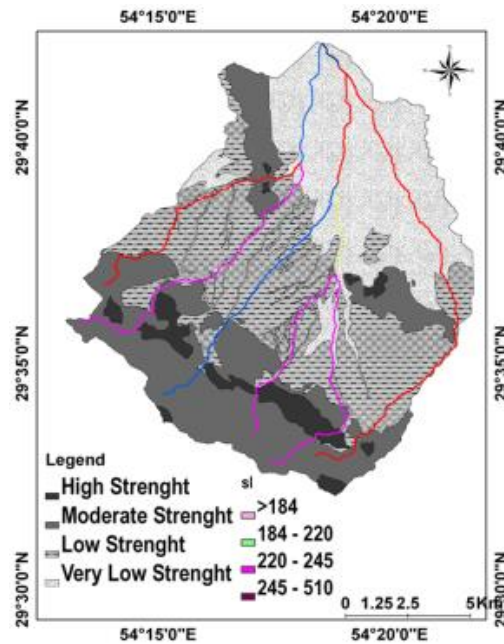


Fig. 2. Geological strength levels and distribution of SL index anomalies for Shahriary basin

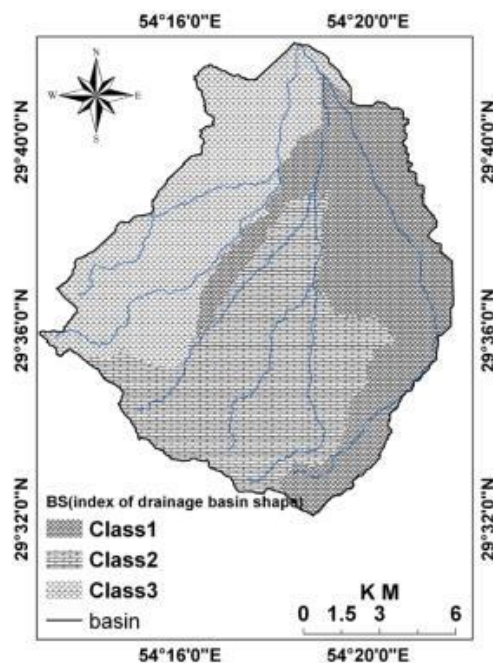


Fig. 3. Variation of the Bs index in the study area

The  $H_i$  correlated with the tectonic activity in the uplifted areas and was 0.56, 0.52 and 0.45 in the G, I and A sub-catchments, respectively. These values agreed with the evidence for maximum geological strength and uplift in the sub-catchments. For example, the steepest cliffs were found within the southern sub-catchments (Fig. 6).

The IRAT groups (Fig. 7) at the Shahriary catchment comprised three different classes. The results excluded Class 1 ( $1 < IRAT < 1.5$  or very high tectonic activity) in the study area. In contrast, an area of 112.15 km<sup>2</sup>, which corresponded to 71.37% of the study area, was categorized as Class 2 ( $1.5 < IRAT < 2$ ). Therefore, the Shahriary basin was identified as a tectonically active basin. Furthermore, 19% of the catchment area was identified as Class 3 ( $2 < IRAT < 2.5$ ), which indicated a moderate tectonic risk. Table 1 presents the RAT index classifications for the eight sub-catchments in the study area.

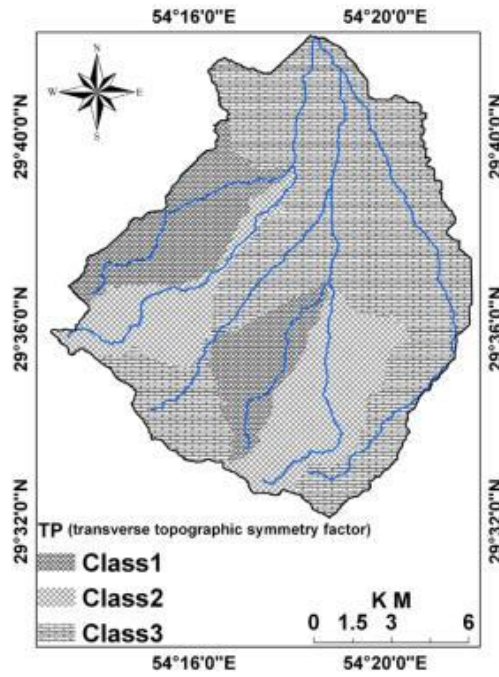


Fig. 4. The Tp map of Shahriary catchment

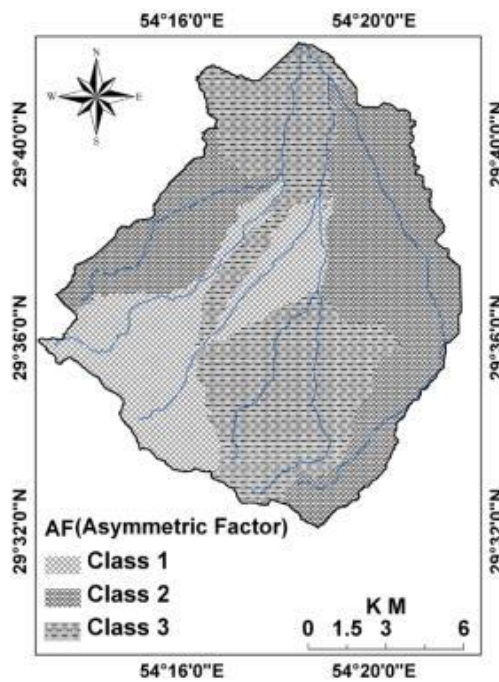


Fig. 5. The distribution of the asymmetric factor map of Shahriary catchment

Table 1. Classification of IRAT in the Shahriary catchment

No	Sub Catchments	Geomorph Indices					S/N	Class	Classification
		HI	BS	TP	AF	SL			
1	J	1	2	2	3	3	2.2	3	Moderate
2	I	1	2	1	3	3	2	2	High
3	E	1	2	3	1	3	2	2	High
4	G	1	3	2	1	2	1.8	2	High
5	D	1	3	1	2	3	2	2	High
6	F	1	1	3	3	3	2.2	3	Moderate
7	C	1	1	3	2	3	2	2	High
8	A	1	3	3	3	3	2.6	4	Low



Fig. 6. The cliff view of rock units at the south of the study area

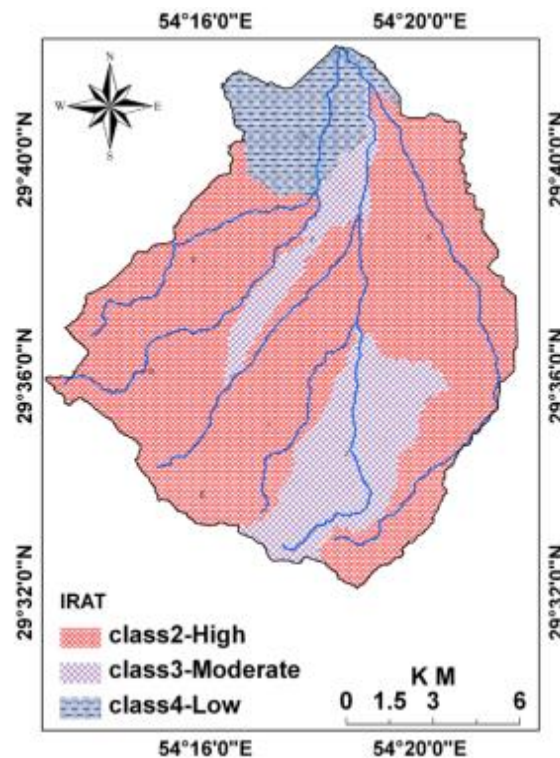


Fig. 7. Distribution classes of relative tectonic activity index (IAT)

#### 4. 2. Geological evidence

Field observations indicated that the fault ruptures in the study area represented the secondary order of the main faulting trends in the Zagros collision province. A total of 42 faults and lineation were surveyed in the study area. Superficial rupture of the longest fault had a length of 11 km. This fault was a dip-slip fault parallel to the shortening mechanism of the Zagros collision zone. Additional fault trends occurred at right angles to the main trend and followed a strong dip-slip mechanism. These faults were mainly contributed to uplifting and the development of alluvial fans, cliffs and steep hills. In addition, this evidence highlighted the tectonic movements during the quaternary period.

This research elucidates the evolutionary trends of joints and failures in rock units. Several failures and a large number of fault junctions appeared in the stratigraphic units of the basin. The results indicated an increase in the frequency and distribution of faults and surface ruptures in the Devonian rock units. On the other hand, these rock units experienced tectonic effects, especially from Cimmerian orogenic events. Superficial rupture trends (mostly in the N45 direction) which developed in the Devonian rock unit are shown in Figure 8a. However, more recent tectonic movements could result in the development of further lineation and surface failures (Fig. 9b, c and d).

The IRAT was evaluated base on seismicity characteristics (Table 2) and geomorphic indices. The potential seismicity was calculated by adopting the methods of Mohajer-Ashjaei and Nowroozi (1978), Nowroozi (1985) and Wells and Coppersmith (1994). The maximum, minimum and mean  $M_s$  values were 5.62, 4.16, and 4.8 (Ms), respectively, based on the method of Mohajer-Ashjaei and Nowroozi (1978). These parameters were 5.89, 4.35, and 4.99 (Ms), respectively, according to the method of Nowroozi (1985). Similarly, the maximum, minimum, and mean earthquake magnitudes of 5.62, 4.16 and 4.8 Ms were based on the method of Wells and Coppersmith (1994). The mean earthquake magnitude at the Shahriary basin was  $4.8 \pm 0.2$  Ms. Thirty-eight recorded earthquakes, with estimated earthquake magnitudes, were reported in the Shahriary area, thus indicating that Shahriary is a low to moderate risk area.

According to Gharibreza et al. (2009), 38 earthquake epicenters occurred near the Shahriary catchment. The magnitude of recorded earthquakes ranged between 6 and 4 Ms. These earthquakes occurred between 75 and 10 km from the catchment area. The seismic hazard zonation map of Iran (IIEES, 1995) indicated an acceleration gravity of 30% for the Shahriary area. A return period of 75 years was used to calculate the frequency, and this resulted in a 50% probability of increased occurrence in 50 years. Therefore, the Shahriary catchment is expected to be a high-risk area for earthquakes. In addition, this research identified a gap in previous studies (Negareh, 2003; Yamani et al., 2011; Madadi et al., 2005; Goorabi, 2007; Habibollah, 2007; Mokhtari, 2005; Khosravi, 2008; Khatib, 2008; Karami, 2009; Zare-Mehrjerdi, 2012) regarding the need for confirmation with geological evidence and seismicity indices. Therefore, the earthquake magnitudes were assessed by using the surface rupture length. In addition, other qualified methods were used to verify the geomorphic indices. Therefore, application of the

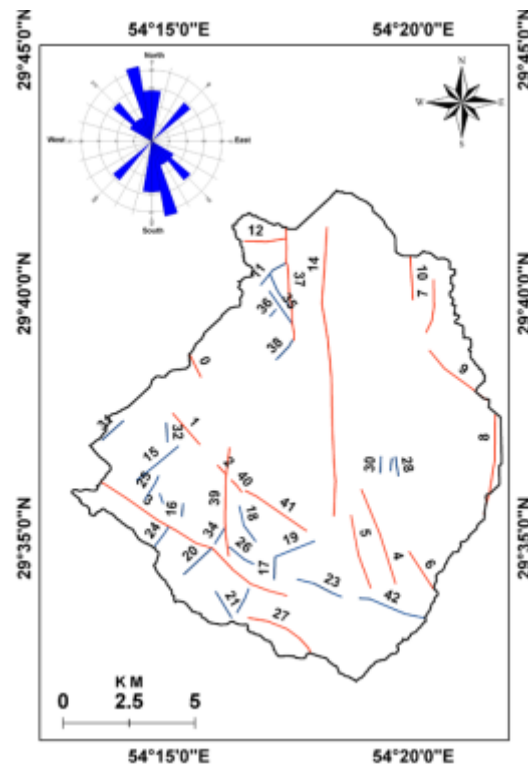


Fig. 8. Distribution classes of relative tectonic activity index (IAT)

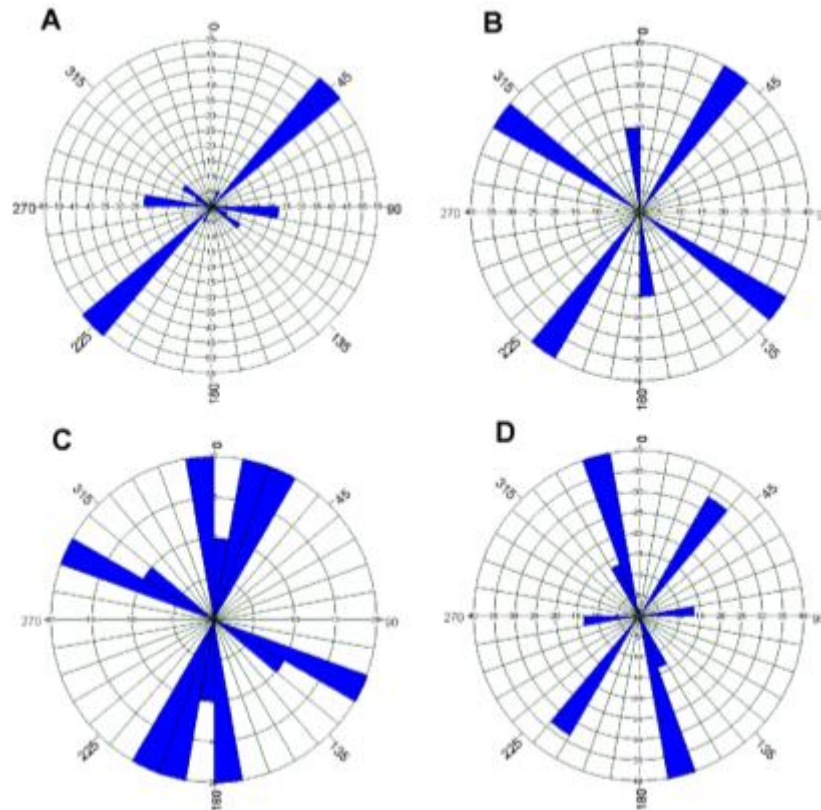


Fig. 9. Direction and frequency of fractures in the Shahriary catchment

Table 2. Estimation of earthquake magnitude based on the surface rupture length

Fault No.	Fault length (km)	<i>Seismicity of faults (Ms)</i>		
		Ashjaei & Nowroozi (1978)	Nowroozi (1985)	Wells & Coppersmith 1994
0	0.98	4.57	4.33	4.74
1	1.50	4.75	4.56	4.94
2	0.41	4.19	3.86	4.35
3	7.62	5.46	5.44	5.69
4	3.76	5.15	5.06	5.36
5	2.86	5.03	4.91	5.24
6	1.64	4.79	4.61	4.98
7	2.05	4.89	4.73	5.08
8	3.80	5.16	5.06	5.37
9	2.71	5.01	4.88	5.21
10	1.65	4.79	4.61	4.98
11	1.22	4.66	4.45	4.85
12	1.40	4.72	4.52	4.91
13	1.41	4.73	4.53	4.91
14	11.04	5.62	5.64	5.86
15	1.91	4.86	4.69	5.05
16	0.51	4.28	3.98	4.45
17	0.85	4.51	4.25	4.68
18	1.49	4.75	4.56	4.94
19	1.46	4.74	4.54	4.93
20	1.37	4.71	4.51	4.90
21	1.14	4.63	4.41	4.81
22	1.02	4.58	4.35	4.76
23	1.65	4.79	4.61	4.98
24	0.88	4.52	4.27	4.70
25	1.04	4.59	4.36	4.77
26	1.06	4.60	4.37	4.78
27	2.60	4.99	4.86	5.19
Max	11.04	5.62	5.64	5.89
Min	0.41	4.19	3.86	4.35
Ave	2.179	4.80	4.61	4.99

proposed method for assessing the IRAT of an area is confidently recommended in watershed management planning.

The resultant data revealed that there exists a clear correlation between geomorphic indices and geological phenomenon. The highest value of the SL index was obtained in areas having rock units with the greatest geological strength (Class 2). Additionally, the longest fault dictated the increase in the Bs index ( $B_s > 4$ ) in the elongated shape sub-catchment. Accordingly, the most effectiveness of tectonic activities was expected in such sub-catchments. Similarly, the highest value of transverse topographic symmetry factor (Tp) correlated with Bs values where the longest fault existed. On the other hand, maximum factor of asymmetry clearly correlated with the most folded and uplifted rock units. The results demonstrated the ability of geomorphic indices to reveal tectonic situation of the Shahriary area. This catchment was identified as a tectonically active basin.

An overall view of tectonic evidences like operation of faulting and folding showed that these have mainly contributed in the uplifting of rock units and the development of alluvial fans, cliffs and steep hills, especially during the quaternary period. In other words, morphological aspects of Shahriary area could be classified in morphotectonic landforms. Such landforms were tectonically active on the basis of pattern of regional movements of major faults and shortening axes of earth crust.

The present research has confidently introduced a comprehensive method for estimation of the relative active tectonics and geo-hazards of an area. This method categorized the Shahriary area as highly risked by geomorphic indices, which were confirmed by seismicity indices. Geo-hazard potential of the study area was compatible with the regional seismic hazard zonation map of Iran. Thus, the geomorphic index data were verified based on the geological evidence and local landforms. Therefore, the IRAT, which is a consequent geomorphic index, brought vital advantages for decision makers in terms of suitable practices for water and soil resources protection.

## 5. Conclusions

The Shahriary catchment represents several tectonic-induced landforms that can be useful in evaluating the IRAT with geomorphic indices. This research emphasized the use of seismicity indices in order to confirm the IRAT index with geomorphic indices. Accordingly, the SL, Af, Hi and Tp were used to prepare a map of the IRAT groups. The IRAT mapping highlighted the distribution of strong tectonic evidences for more than 70% of the study area. Several landforms, such as extremely uplifted rock, dip-slip hills, cliffs, and coarse-grained alluvial fans, supported these results. The application of well-tested empirical methods for estimating the earthquake magnitude and gravity acceleration suggested that the Shahriary catchment has a moderate earthquake risk. Consequently, the integrated method involves the use of geomorphic indices and geological evidence in estimating the relative tectonic activity of an area.

## References

1. Alipoor, R., Poorkermani, M., Zare, M., El-Hamdouni, R., 2011. Active tectonic assessment around Rudbar Lorestan dam site, High Zagros Belt (SW of Iran). *Geomorphology*, 128, 1-14.
2. Azor, A., Keller, E.A., Yeats, R.S., 2002. Geomorphic indicators of active fold growth: South Mountain–Oak Ridge Ventura basin, southern California. *American Bulletin*, 114, 745-753.
3. Bull, W.B., McFadden, L.D. 1977. Tectonic geomorphology north and south of the Garlock fault. *Proceedings of the 8<sup>th</sup> Annual Geomorphology Symposium*, Binghamton, State University of New York.
4. Cannon, P.J., 1976. Generation of explicit parameters for a quantitative geomorphic study of Mill Creek drainage basin. *Geology Notes*, 36 (1), 3–16.
5. Della Seta, M., Del-Monte, M., Fredi, P., Miccadei, E., Nesci, O., Pambianchi, G., Piacentini, T., Troiani, F., 2008. Morphotectonic evolution of the Adriatic piedmont of the Apennines: advancement in the knowledge of the Marche–Abruzzo border area. *Geomorphology*, 102, 119–129.
6. El-Hamdouni, R., Irigaray, C., Fernández, T., Chacón, J., Keller, E.A., 2008. Assessment of

- relative active tectonics, southwest border of the Sierra Nevada (southern Spain). *Geomorphology*, 96, 150–173.
7. Gharibreza, M., Masoumi, H., Habibi, A., 2009. Geology and Geomorphology of Shahriari Catchment. Tehran. Soil Conservation and Watershed Management Research Institute, 114.
  8. Ghorabi, A., 2007. Evidences of Active Geomorphology of Darake Basin. *Geography Research*, 60, 177-196.
  9. Habibollahi, M., 2007. Analysis of Active Tectonic in Zayandehrod Upstream. *Geography*. Isfahan Isfahan University. M.Sc.
  10. Hack, J.T., 1973. Stream-profiles analysis and stream-gradient index. *Journal of Research of the U.S.*, 1(4), 421–429.
  11. Hare, P.H., Gardner, T.W. 1985. Geomorphic indicators of vertical neotectonism along converging plate margins. *Tectonic Geomorphology*. Proceedings of the 15<sup>th</sup> Annual Binghamton Geomorphology Symposium. Boston, Allen and Unwin.
  12. IIEES 1995. Seismic hazard zonation map of Iran. *Seismology*. Tehran, International Institute of Earthquake Engineering and Seismology.
  13. Karami, F., 2009. Geomorphic assessment of the tectonic activity in the drainage basin saydabad chay. *Physical Geography research*, 69, 67-82.
  14. Keller, E.A., Pinter, N. 2002a. Active Tectonics: Earthquakes, Uplift and Landscape. *Active Tectonics: Earthquakes, Uplift and Landscape*. Newjersey, Prentice Hall.
  15. Khatib, M., 2008. Influence of Nehbandan Fault System on Nehbandan City Morphology. *Geography & Development*, 12, 5-24.
  16. Khosravi, G., 2008. Active Tectonic Analysis and Impact on Drainage Network on Khuzestan Plain. *Geography*. NajafAbad Islamic Azad University. M.Sc.
  17. Madadi, A., Rezaiee, M., Rajaiee, H., 2005. Analysis activity Neo- technique using geomorphological. *Geographical Research*, 2(48), 123-138.
  18. Mahmood, S., Gloaguen, R., 2012. Appraisal of active tectonics in Hindu Kush: Insights from DEM derived geomorphic indices and drainage analysis. *Geoscience Frontiers*, 3(4), 407-428.
  19. Maroukian, H., Gaki-Papana, K., Karymbalis, E., Vouvalidis, K., Pavlopoulos, K., Papanastassiou, 2008. Morphotectonic control on drainage network evolution in thePerachora Peninsula, Greece. *Geomorphology*, 102, 81–92.
  20. Mayer, L., 1990. Introduction to Quantitative Geomorphology. Newjersey, Prentice Hall, Englewood, Cliff.
  21. Mohajer-Ashjai, A., Nowroozi, A.A., 1979. The Tabas earthquake of September 16, 1978 in eastcentral Iran: a preliminary field report. *Geophysics Research Letters*, 6, 689-692.
  22. Mokhtari, D., 2005. Morph metric parameters used in determining the amount of activity faults (A case study: North fault Mishoo). *Earth Sciences*, 59, 70-83.
  23. Molin, P., Pazzaglia, F.J., Dramis, F., 2004. Geomorphic expression of active tectonics in a rapidly-deforming forearc, sila massif, Calabria, southern Italy. *American Journal of Science*, 304, 559–589.
  24. Negaresh, H., 2003. Earthquake, Cites, and Faults. *Geography Researches*, 1, 1-18.
  25. Nowroozi, A.A., 1985. Empirical relations between magnitudes and fault parameters for earthquakes in Iran. *Bulletin of the Seismological Society of America (BSSA)*, 75, 1327-1338.
  26. Paul, A., Hatzfeld, D., Kaviani, A., Tatar, M., Péquegnat, C., 2010. Seismic imaging of the lithospheric structure of the Zagros mountain belt (Iran). *Geomorphology*, 330, 5-18.
  27. Pike, R.J., Wilson, S.E., 1971. Elevation–relief ratio, hypsometric integral and geomorphic area-altitude analysis. *Geological Society of America Bulletin*, 82, 1079–1084.
  28. Ramírez-Herrera, M., 1998. Geomorphic assessment of active tectonics in the Acambay Graben, Mexican volcanic belt. *EarthSurface Processes and Landforms*, 23, 317–332.
  29. Silva, P.G., Goy, J.L., Zazo, C., Bardajm, T., 2003. Fault generated mountain fronts in Southeast Spain: geomorphologic assessment of tectonic and earthquake activity. *Geomorphology*, 250, 203–226.
  30. Strahler, A.N., 1952. Hypsometric (area-altitude) analysis of erosional topography. *Geological Society of America Bulletin*, 63, 1117–1142.
  31. Troiani, F., Della-Seta, M., 2008. The use of the stream length–gradient index in

- morphotectonic analysis of small catchments: A case study from Central Italy. *Geomorphology*, 102, 159–168.
32. Wells, D.L., Coppersmith, K.J., 1994. New Empirical Relationships among Magnitude, Rupture Length, Rupture Width, Rupture Area, and Surface Displacement. *Bulletin of the Seismological Society of America*, 84(4), 974-1002.
  33. Yamani. M.B.S., JafariAghdam, M. 2011. Impact Neo tectonic in the morphology Drainage basin Western Zagros. *Geographical environment*, 1, 68-82.
  34. Zare-Mehrjerdi, A.A., 2012. Zonation of west Alborz zone based on geomorphic indices. *Geography and Environmental Planning*, 45, 49-51.
  35. Obruchev, V.A., 1948. "Osnovnye cherty kinetiki i plastiki neotektonik". *Izv. Akad. Nauk, Ser. Geol.*, 5: 13–24.
  36. Mandl, G., 2005. *Rock Joints: The Mechanical Genesis*. Springer-Verlag, Heidelberg, Germany. 221 pp.